Arab J Sci Eng (2014) 39:1261–1270
DOI 10.1007/s13369-013-0717-8

RESEARCH ARTICLE - MECHANICAL ENGINEERING

Thermally Developing Flow Induced by Electro-Osmosis in a Circular Micro-Channel

Ali Jabari Moghadam

Received: 9 March 2012 / Accepted: 9 July 2013 / Published online: 5 September 2013

Abstract The steady-state electro-kinetic-driven flow and heat transfer in circular micro-channels are studied under hydrodynamic fully developed and thermally developing conditions. Based on the linearized Poisson–Boltzmann equation, an exact solution of the electrical potential distribution is obtained. The analytic solutions of the velocity and temperature profiles are then obtained, and the effects of some hydrodynamic and thermal parameters on flow and heat transfer are investigated. The interesting plug-like velocity profile produced by external electrical field is not usually observed in the pressure-driven flows. In this case, the very large velocity gradient near the wall of the micro-channel may result in the enhanced temperature close to the wall (depending on the relative importance of viscous dissipation compared with the other terms); the temperature values of other portions of the flow field are increased slightly. Decreasing both Reynolds and Prandtl numbers leads to increasing the bulk fluid temperature. Nusselt number decreases in the thermally developing region.

Keywords Electro-osmotic flow · Thermally developing region · Circular micro-channel · Plug-like velocity profile · Nusselt number

A. J. Moghadam (✉)
Department of Mechanical Engineering, Shahrood University of Technology, Post Box 316, Shahrood, Iran
e-mail: jm.ali.project@gmail.com

الخلاصة

تمت ـ في هذه الورقة العلمية ـ دراسة التدفق المدفوع كهربائيا، وحركيا في الحالة المستقرة، ونقل الحرارة في قنوات دائرية متناهية الصغر تحت الظروف الهيدروديناميكية متكاملة النمو والظروف الحرارية النامية. واستنادا إلى معادلة بواسون بولتزمان الخطية تم الحصول على الحل الدقيق لتوزيع الجهد الكهربائي. وتم ـ بعد ذلك ـ الحصول على الحلول التحليلية للسرعة، وملامح درجة الحرارة، والتحقيق في آثار بعض المعاملات الهيدروديناميكية والحرارية على تدفق وانتقال الحرارة. إن نمط السرعة مثل القابس المثير للاهتمام والمنتج بمجال كهربائي خارجي لا يلاحظ عادة في التدفقات المدفوعة بالضغط. وفي هذه الحالة، فإن التدرج الكبير جدا في السرعة بالقرب من جدار القناة متناهية الصغر يؤدي إلى تعزيز درجة الحرارة القريبة من الجدار (اعتمادا على الأهمية النسبية للتبديد اللزج مقارنة بمصطلحات أخرى)، وقيم درجة الحرارة من أجزاء أخرى من مجال التدفق ازدادت قليلا. إن خفض أعداد رينولدز وبراندتل يؤدي إلى زيادة درجة حرارة معظم السائل، ويقل عدد نسلت في المنطقة النامية حراريا.

List of Symbols

c_p	Specific heat (J/kg K)
e	Electron charge (C)
E_z	Dimensionless electrical field strength
Ek	Eckert number
F_z	Dimensionless electrical force per unit volume
h_z	Local convection heat transfer coefficient (W/m^2 K)
$I_\nu(x)$	Modified Bessel function of the first kind and order ν
k_B	Boltzmann constant (J/K)
k_f	Fluid thermal conductivity (W/m K)
L	Length of channel (m)
M	Ratio of electrical to frictional forces
n_0	Bulk ion concentration (m^{-3})
Nu	Nusselt number
Pe	Peclet number
Pr	Prandtl number
q''	Dimensionless heat flux
r	Dimensionless radial coordinate

R	Radius of the micro-channel (m)
Re	Reynolds number
s	Ratio of half channel diameter to Debye length
T	Dimensionless temperature
$T_{\mathrm{m}}(z)$	Local mean fluid temperature (K)
T_{s}	Constant wall temperature (K)
U	Reference velocity (m/s)
V_z	Dimensionless axial velocity
z	Dimensionless axial coordinate
$\mathbb{Z}$	Valence of ionic species

Greek Symbols

ε	Electric permittivity of solution (F/m)
κ	Debye–Huckel parameter (m^{-1})
λ	Eigenvalue
μ	Dynamic viscosity (kg/m s)
ρ	Fluid density ($\mathrm{kg/m}^3$)
ρ_e	Net volume charge density ($\mathrm{C\ m}^{-3}$)
ψ	Dimensionless electrical potential
ζ	Dimensionless zeta potential at the wall

Subscript

m	Mean value

Superscript

$*$	Dimensional quantities

1 Introduction

A lab-on-a-chip device has a network of micro-channels, electrodes, sensors and electrical circuits. Electrodes are placed at strategic locations on a chip. Applying electrical fields along micro-channels controls the liquid flow and other operations in the chip. Hence, understanding the electro-osmotic flow in micro-channels is essential to controlling the key micro-fluidic processes and designing them systematically.

Because all solid–liquid (aqueous solutions) interfaces carry electrostatic charges, there is an electrical double layer (EDL) field in the region close to the solid–liquid interface on the liquid side. In the electro-osmosis phenomenon which is due to an EDL field, there is the liquid motion caused by interaction between the EDL at the liquid-channel wall interface with an electrical field applied tangentially to the wall. Immediately, next to the solid surface, there is a layer of ions that are strongly attracted to the solid surface and are immobile. This layer is called the compact layer, normally about several Angstroms thick. Because of the electrostatic attraction, the counterions concentration near the solid surface is higher than that in the bulk liquid far away from the solid surface. The coions concentration near the surface, however, is lower than that in the bulk liquid far away from the solid surface, due to the electrical repulsion. So there is a net charge in the region close to the surface. From the compact layer to the uniform bulk liquid, the net charge density gradually reduces to zero. Ions in this region are affected less by the electrostatic interaction and are mobile. This region is called the diffuse layer of the EDL. The thickness of the diffuse layer is dependent on the bulk ionic concentration and electrical properties of the liquid, usually ranging from several nanometers for high ionic concentration solutions up to several microns for pure water and pure organic liquids. The boundary between the compact layer and the diffuse layer is usually referred to as the shear plane. The electrical potential at the shear plane is called the zeta potential ζ and can be measured experimentally. In practice, the zeta potential is used as an approximation to the potential at the solid–liquid interface. If an electric field is applied along the length of a channel, an electrical body force is exerted on the ions in the diffuse layer. In the diffuse layer of the EDL field, the net charge density ρ_e is not zero. The net transport of ions is the excess counterions. If the solid surface is negatively charged, the counterions are the positive ions. These excess counterions will move under the influence of the applied electrical field, pulling the liquid with them and resulting in electro-osmotic flow. The liquid movement is carried through to the rest of the liquid in the channel by viscous forces.

In most lab-on-a-chip applications, the electro-osmotic flow is preferred over the pressure-driven flow. One of the reasons is the plug-like velocity profile of the electro-osmotic flow. That is, fluid samples can be transported without dispersion caused by flow shear. The second reason is that pumping a liquid through a very small channel requires applying a very large pressure difference depending on the flow rate. This is often impossible because of the limitations of the size and mechanical strength of the micro-fluidic devices. The electro-osmotic flow can generate the required flow rate even in very small micro-channels without any applied pressure difference across the channel. Additionally, using the electro-osmosis phenomenon to transport liquids in a complicated micro-channel network does not require any external pump or moving parts, but it may be controlled by the electrical fields via electrodes. Although high voltages are often necessary in electro-osmotic flows, the required electrical power is very small due to the very low current involved. However, heat generated in the electro-osmotic flow eventually presents problems to many applications where solutions of high electrolyte concentrations and long operation time are required [1].

Over the last two decades, developments in micro-fabrication technologies have enabled many different types of micro-fluidic systems. Such systems must be understood from an electro-hydrodynamic as well as electro-thermal point of views. Many researchers have studied various features of these phenomena. For example, Anderson [2] studied the particle movement produced by non-uniform

zeta potential in an electric field. Arulanandam and Li [3] studied the liquid movement in a rectangular micro-channel by electro-osmotic pumping. Erickson and Li [4] studied electro-osmotic flow caused by alternative current in a rectangular micro-channel.

Wang and Chen [5] investigated electro-osmosis in homogeneously charged micro- and nano-scale random porous media using mesoscopic simulation methods which involve a random generation-growth method for reproducing three-dimensional random micro-structures of porous media and a lattice Poisson–Boltzmann algorithm for solving the strongly nonlinear governing equations. Dutta and Beskok [6] presented analytical results for velocity distribution, mass flow rate, pressure gradient, wall shear stress, and vorticity in mixed electro-osmotic/pressure driven flows for two-dimensional straight channel geometry. Comprehensive models for a slit channel have also been presented by Dutta and Beskok [7] who developed an analytical model for an applied sinusoidal electric field. Soderman and Jonsson [8] examined the transient flow field caused by a series of different pulse designs. Exact solutions of AC electro-kinetic-driven flow inside circular micro-channels were presented by Moghadam [9] for various periodic functions.

Soong and Wang [10] studied flow and heat transfer between two parallel plates. Xuan and Li [11] presented a thermodynamic analysis on energy conversion due to electro-kinetic flow. Wang and Kang [12] presented a numerical solution based on coupled lattice Boltzmann methods for electro-kinetic flows in micro-channels. Tang et al. [13] investigated the electro-osmotic flow in axisymmetric micro-ducts. They presented axisymmetric lattice Boltzmann models to solve the electric potential distribution and the velocity field. Xuan and Li [14] used a semi-analytical approach to investigate electro-osmotic flows in micro-channels with arbitrary cross-sectional geometry and distribution of wall charge. Sadeghi and Saidi [15] considered the influence of viscous dissipation on thermal transport characteristics of the fully developed, combined pressure and electro-osmotically driven flow in parallel plate micro-channels subject to uniform wall heat flux. Thermally fully developed, electro-osmotically generated convective transport has been analyzed by Maynes and Webb [16] for a parallel plate micro-channel and circular micro-tube. They presented analytical expressions for the fully developed, dimensionless temperature profile and corresponding Nusselt number for both geometric. The effects of the EDL near the solid–liquid interface and the flow-induced electro-kinetic field on the pressure-driven flow and heat transfer through a rectangular micro-channel were reported by Yang et al. [17].

To date, however, less attention has been paid to the thermally developing region of the micro-channels. The objective of this research is to obtain an analytical solution for hydrodynamically developed and thermally developing flow in circular micro-channels, in which the effect of viscous dissipation is also included to determine the temperature profile.

2 Problem Formulation

According to the theory of electrostatics, the Poisson equation describes the relationship between the electrical potential ψ^* and the local net charge density per unit volume ρ_e at any point in the solution [18]:

$$\nabla^2\psi^* = -\frac{\rho_e}{\varepsilon} \tag{1}$$

In which, ε is the dielectric constant of the solution. Assuming the equilibrium Boltzmann distribution equation is applicable, which implies uniform dielectric constant, the number concentration of the type-i ion is of the form:

$$n_i = n_{i0}\exp\left(-\frac{\mathbb{Z}_i e\psi^*}{k_{\mathrm{B}}T^*}\right) \tag{2}$$

where n_{i0} and $\mathbb{Z}_i$ are the bulk ionic concentration and the valence of type-i ions, respectively, e is the charge of a proton, k_{B} is the Boltzmann constant, and T^* is the absolute temperature.

For a symmetric electrolyte ($\mathbb{Z}_- = \mathbb{Z}_+ = \mathbb{Z}$) solution, the net volume charge density ρ_e is proportional to the concentration difference between symmetric cations and anions, via:

$$\rho_e = \mathbb{Z}e(n_+ - n_-) = -2\mathbb{Z}en_0\sinh\left(\frac{\mathbb{Z}e\psi^*}{k_{\mathrm{B}}T^*}\right) \tag{3}$$

Substituting Eq. (3) into the Poisson equation leads to the well-known Poisson–Boltzmann equation:

$$\nabla^2\psi^* = \frac{2\mathbb{Z}en_0}{\varepsilon}\sinh\left(\frac{\mathbb{Z}e\psi^*}{k_{\mathrm{B}}T^*}\right) \tag{4}$$

If we consider the flow is steady and fully developed and there is no pressure gradient in the micro-channel, the general equation of motion is given by a balance between the viscous force in the fluid and the externally imposed electrical field force:

$$\mu\nabla^2 V_z^* = F_z^* \tag{5}$$

where, $F_z^* = \rho_e E_z^*$, E_z^*, μ and V_z^* are the electrical force per unit volume of the liquid, the electric field strength, the fluid viscosity and the fluid axial velocity, respectively. So the above equation is given as follows:

$$\mu\nabla^2 V_z^* = -\frac{2n_\infty\mathbb{Z}e}{\varepsilon\varepsilon_0}\sinh\left(\frac{\mathbb{Z}e}{k_{\mathrm{B}}T^*}\psi^*\right)E_z^* \tag{6}$$

For a thermally developing flow, assuming no axial conduction, the energy equation includes radial conduction and axial advection, together with viscous dissipation [19]:

$$\rho\, c_{\mathrm{p}}\, V_z^*\frac{\partial T^*}{\partial z^*} = k_{\mathrm{f}}\nabla^2 T^* + \mu\Phi^* \tag{7}$$

where, k_f and Φ^* are the fluid thermal conductivity and the viscous dissipation term, respectively. Equations (4), (6) and (7) can be more simplified for the geometry of our problem:

$$\frac{d^2\psi^*}{dr^{*2}} + \frac{1}{r^*}\frac{d\psi^*}{dr^*} = \frac{2\mathbb{Z}en_0}{\varepsilon}\sinh\left(\frac{\mathbb{Z}e\psi^*}{k_B T^*}\right) \tag{8}$$

$$\mu\left(\frac{dV_z^*}{dr^{*2}} + \frac{1}{r^*}\frac{dV_z^*}{dr^*}\right) = -\frac{2n_\infty \mathbb{Z}e}{\varepsilon\varepsilon_0}\sinh\left(\frac{\mathbb{Z}e}{k_B T^*}\psi^*\right)E_z^* \tag{9}$$

$$\rho c_p V_z^*\frac{\partial T^*}{\partial z^*} = k_f\left[\frac{1}{r^*}\frac{\partial}{\partial r^*}\left(r^*\frac{\partial T^*}{\partial r^*}\right)\right] + \mu\left(\frac{dV_z^*}{dr^*}\right)^2 \tag{10}$$

Equations (8), (9) and (10) are the governing equations of the electro-kinetic flow and heat transfer in circular micro-channels, subject to the following boundary conditions:

$$\begin{cases} r^* = 0 \ : \dfrac{\partial\psi^*}{\partial r^*} = 0 \\ r^* = R : \psi^* = \zeta^* \end{cases} \tag{11}$$

$$\begin{cases} r^* = 0 \ : \dfrac{dV_z^*}{dr^*} = 0 \\ r^* = R : V_z^* = 0 \end{cases} \tag{12}$$

$$\begin{cases} r^* = 0 \ : \dfrac{\partial T^*}{\partial r^*} = 0 \\ r^* = R : T^* = T_s \end{cases}, \quad z^* = 0 : T^* = T_i \tag{13}$$

where, R, T_s, T_i and ζ^* are the micro-channel radius, surface temperature, fluid inlet temperature into the channel and zeta potential value at the surface, respectively.

Now by introducing the following dimensionless variables:

$$\begin{gathered} r = \frac{r^*}{R}, \quad z = \frac{z^*}{L}, \quad \psi = \frac{\mathbb{Z}e}{k_B T}\psi^*, \ V_z = \frac{V_z^*}{U} \\ E_z = \frac{E_z^* L}{\zeta^*}, \quad T = \frac{T^* - T_s}{\Delta T} \ \text{where}, \quad \Delta T = T_s - T \end{gathered} \tag{14}$$

into Eqs. (8)–(13), the governing equations and boundary conditions in non-dimensional form can be achieved. Quantities U and L are the reference velocity and length of the channel (or distance between electrodes), respectively.

$$\frac{d^2\psi}{dr^2} + \frac{1}{r}\frac{d\psi}{dr} = (\kappa R)^2\sinh\psi \tag{15}$$

$$\frac{d^2V_z}{dr^2} + \frac{1}{r}\frac{dV_z}{dr} = -M\,E_z\sinh\psi \tag{16}$$

$$V_z\frac{\partial T}{\partial z} = \frac{1}{Pe}\left[\frac{1}{r}\frac{\partial}{\partial r}\left(r\frac{\partial T}{\partial r}\right)\right] + \frac{Ek}{Re}\left[\left(\frac{dV_z}{dr}\right)^2\right] \tag{17}$$

$$\begin{cases} r = 0 : \dfrac{\partial\psi}{\partial r} = 0 \\ r = 1 : \psi = \zeta \end{cases} \tag{18}$$

$$\begin{cases} r = 0 : \dfrac{dV_z}{dr} = 0 \\ r = 1 : V_z = 0 \end{cases} \tag{19}$$

$$\begin{cases} r = 0 : \dfrac{\partial T}{\partial r} = 0 \\ r = 1 : T = 0 \end{cases}, \quad z = 0 : \quad T = -1 \tag{20}$$

where, κ, the Debye–Huckle parameter, is defined as follows:

$$\kappa = \left(\frac{2\mathbb{Z}^2 e^2 n_\infty}{\varepsilon\varepsilon_0 k_B T}\right)^{1/2} \tag{21}$$

and $1/\kappa$ is the characteristic thickness of the EDL. The non-dimensional parameter κR is a measure of the relative channel diameter, compared to the EDL thickness. κR is often referred to as the electro-kinetic diameter. The parameter M is a new dimensionless group, which is a ratio of the electrical force to the frictional force per unit volume, given by:

$$M = \frac{2n_\infty \mathbb{Z}\,e\,\zeta^* R^2}{\mu\,U\,L\,\varepsilon\,\varepsilon_0} \tag{22}$$

The dimensionless parameters, named Reynolds number, Prandtl number, Peclet number and Eckert number are also defined as follows:

$$\begin{gathered} Re = \frac{\rho\,U(R^2/L)}{\mu}, \quad \Pr = \frac{\nu}{\alpha}, \quad Pe = Re\,\Pr, \\ Ek = \frac{U^2}{c_p\Delta T}. \end{gathered} \tag{23}$$

3 Solution Procedure

The solution method presented here is valid for small values of ψ, for which we have $\sinh\psi \cong \psi$, so in Eqs. (15)–(17), $\sinh\psi$ is replaced by ψ for the next mathematical operations. By this approximation, Eq. (15) is a linear homogeneous ODE, and its solution subject to the boundary conditions (18) is given as:

$$\psi(r) = \frac{\zeta}{I_0(s)}I_0(sr) \tag{24}$$

where, $s = \kappa R$ is the ratio of half channel diameter to Debye length (the length scale ratio), and $I_\nu(x)$ is the modified Bessel function of the first kind satisfying the following modified Bessel function [20]:

$$x^2y'' + x\,y' - (x^2 + v^2)y = 0 \tag{25}$$

Equation (16) is a linear non-homogeneous ODE, and its solution subject to the boundary conditions (19) is now found as follows:

$$V_z(r) = \frac{M\,E_z\,\zeta}{s^2}\left[1 - \frac{I_0(sr)}{I_0(s)}\right] \tag{26a}$$

$$V = \frac{V_z(r)}{\left(\frac{M\,E_z\,\zeta}{s^2}\right)} = 1 - \frac{I_0(sr)}{I_0(s)} \tag{26b}$$

The dimensionless velocity profiles for different values of s in the form of Eq. (26b) can achieve unity in the middle of the channel.

The energy Eq. (17) is a linear non-homogeneous partial differential equation, in which, the r-dependent viscous

dissipation term is the non-homogeneity term. To solve this equation by the method of separation of variables, we have to get rid of the non-homogeneity term. Since Eq. (17) is linear, we can solve it by introducing the following superposition:

$$T(r,z) = \theta(r,z) + \phi(r) \tag{27}$$

Then Eq. (17) can be divided into the following two equations:

$$V_z \frac{\partial \theta}{\partial z} = \frac{1}{Pe}\left[\frac{1}{r}\frac{\partial}{\partial r}\left(r\frac{\partial \theta}{\partial r}\right)\right] \tag{28}$$

$$\frac{1}{Pe}\left[\frac{1}{r}\frac{\mathrm{d}}{\mathrm{d}r}\left(r\frac{\mathrm{d}\phi}{\mathrm{d}r}\right)\right] + \frac{Ek}{Re}\left[\left(\frac{\mathrm{d}V_z}{\mathrm{d}r}\right)^2\right] = 0 \tag{29}$$

The corresponding boundary equations are as follows:

$$\frac{\partial \theta}{\partial r}(0,z) = 0, \quad \theta(1,z) = 0, \quad \theta(r,0) = -1 - \phi(r) \tag{30}$$

$$\frac{\mathrm{d}\phi}{\mathrm{d}r}(0) = 0, \quad \phi(1) = 0 \tag{31}$$

Solution of (29) subject to (31) is given here by an infinite series truncated up to order 10:

$$\phi(r) = \frac{1}{4}\frac{Pe\,Ek\,M^2 Ez^2\zeta^2}{Re\,[I_0(s)]^2}\left\{\begin{array}{l}\frac{1}{16}(1-r^4)+\frac{1}{144}s^2(1-r^6)\\ +\frac{5}{12288}s^4(1-r^8)\end{array}\right\} + O(r^{10}) \tag{32}$$

To solve Eq. (28) subject to the boundary conditions (30), the separation of variables method is employed. If the following product form:

$$\theta(r,z) = A(r)B(z) \tag{33}$$

is substituted into Eq. (28), the following equality will be obtained:

$$\underbrace{\frac{1}{V_z A}\left(\frac{\mathrm{d}^2 A}{\mathrm{d}r^2} + \frac{1}{r}\frac{\mathrm{d}A}{\mathrm{d}r}\right)}_{\text{function of } r} = \underbrace{\frac{Pe}{B}\frac{\mathrm{d}B}{\mathrm{d}z}}_{\text{function of } z} \equiv \text{constant} = -\lambda \tag{34}$$

This separation constant is negative, since the boundary conditions in radial direction:

$$A'(0) = 0, \quad A(1) = 0 \tag{35}$$

are homogeneous. The ordinary differential equations resulted from (34) are:

$$\frac{\mathrm{d}^2 A}{\mathrm{d}r^2} + \frac{1}{r}\frac{\mathrm{d}A}{\mathrm{d}r} + \lambda\, V_z\, A = 0 \tag{36}$$

$$\frac{\mathrm{d}B}{B} = -\frac{\lambda}{Pe}\mathrm{d}z \tag{37}$$

Solution of Eq. (36) subject to the first condition of (35) is given by an infinite series as follows:

$$A(r) = c_1\left\{\begin{array}{l}1 - \frac{1}{4}\frac{\lambda\, M\, Ez\,\zeta\,[I_0(s)-1]}{s^2 I_0(s)} r^2\\ +\frac{1}{64}\frac{\lambda\, M\, Ez\,\zeta}{s^4\,[I_0(s)]^2}\left[\begin{array}{l}\lambda\, M\, Ez\,\zeta - 2\lambda\, M\, Ez\,\zeta\, I_0(s)\\ +\lambda\, M\, Ez\,\zeta\,[I_0(s)]^2 + s^4 I_0(s)\end{array}\right] r^4\\ -\frac{1}{2304}\frac{\lambda\, M\, Ez\,\zeta}{s^6\,[I_0(s)]^3}\left[\begin{array}{l}-5\lambda\, M\, Ez\,\zeta\, s^4 I_0(s) + 5\lambda\, M\, Ez\,\zeta\,[I_0(s)]^2 s^4\\ -\lambda^2 M^2 Ez^2\zeta^2 + 3\lambda^2 M^2 Ez^2\zeta^2 I_0(s)\\ -3\lambda^2 M^2 Ez^2\zeta^2\,[I_0(s)]^2\\ +\lambda^2 M^2 Ez^2\zeta^2\,[I_0(s)]^3 - s^8\,[I_0(s)]^2\end{array}\right] r^6\\ +\frac{1}{147456}\frac{\lambda\, M\, Ez\,\zeta}{s^8\,[I_0(s)]^4}\left[\begin{array}{l}14\lambda^2 M^2 Ez^2\zeta^2 s^4 I_0(s)\\ -28\lambda^2 M^2 Ez^2\zeta^2\,[I_0(s)]^2 s^4\\ +14\lambda^2 M^2 Ez^2\zeta^2\,[I_0(s)]^3 s^4\\ +19\lambda M\, Ez\,\zeta\, s^8\,[I_0(s)]^2 + (\lambda\, M\, Ez\,\zeta)^3\\ -4(\lambda\, M\, Ez\,\zeta)^3 I_0(s)\\ +6(\lambda\, M\, Ez\,\zeta)^3\,[I_0(s)]^2\\ -4(\lambda\, M\, Ez\,\zeta)^3\,[I_0(s)]^3\\ +(\lambda\, M\, Ez\,\zeta)^3\,[I_0(s)]^4\\ -10\lambda\, M\, Ez\,\zeta\,[I_0(s)]^3 s^8 + s^{12}\,[I_0(s)]^3\end{array}\right] r^8 + O(r^{10})\end{array}\right\} \tag{38}$$

where, c_1 is a constant, and the solution is up to order 10 for more accuracy. Using the second condition of (35), we have the eigenvalues λ_n, for $n = 1, 2, \ldots$. Solution of Eq. (37) is:

$$B(z) = c_2\, \exp\left(-\frac{\lambda}{Pe}z\right) \tag{39}$$

By considering the above functions for the whole range of eigenvalues, $A(r)$ and $B(z)$ are written in a simple form:

$$\begin{aligned} A_n(r) &= c_{1n}\, f_n(r)\\ B_n(z) &= c_{2n}\, g_n(z)\end{aligned} \tag{40}$$

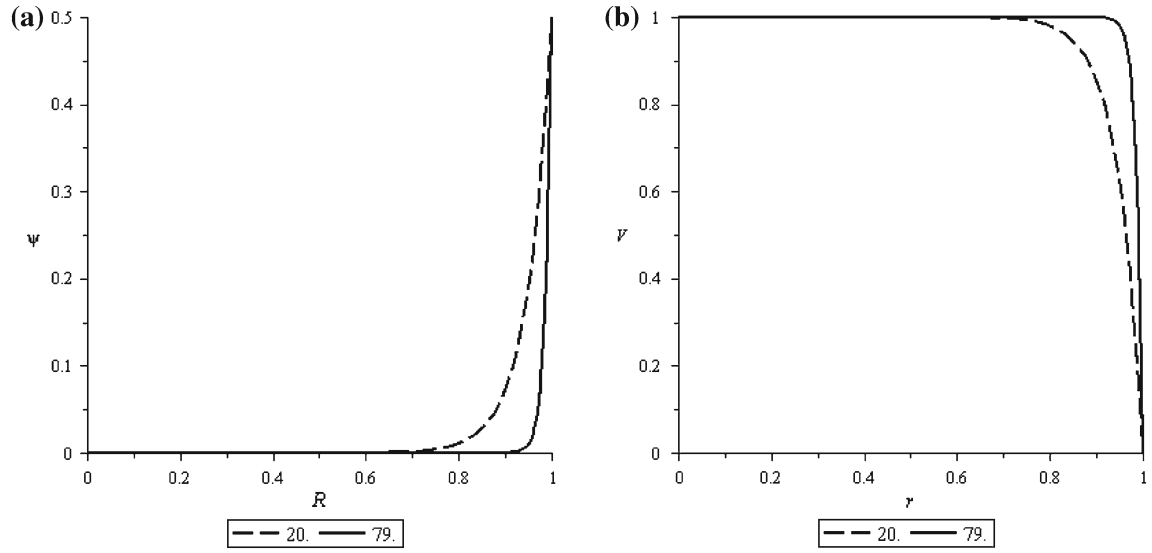

Fig. 1 **a** Dimensionless electrical potential, and **b** dimensionless velocity distributions for $\zeta = 0.5$ and two different values of s

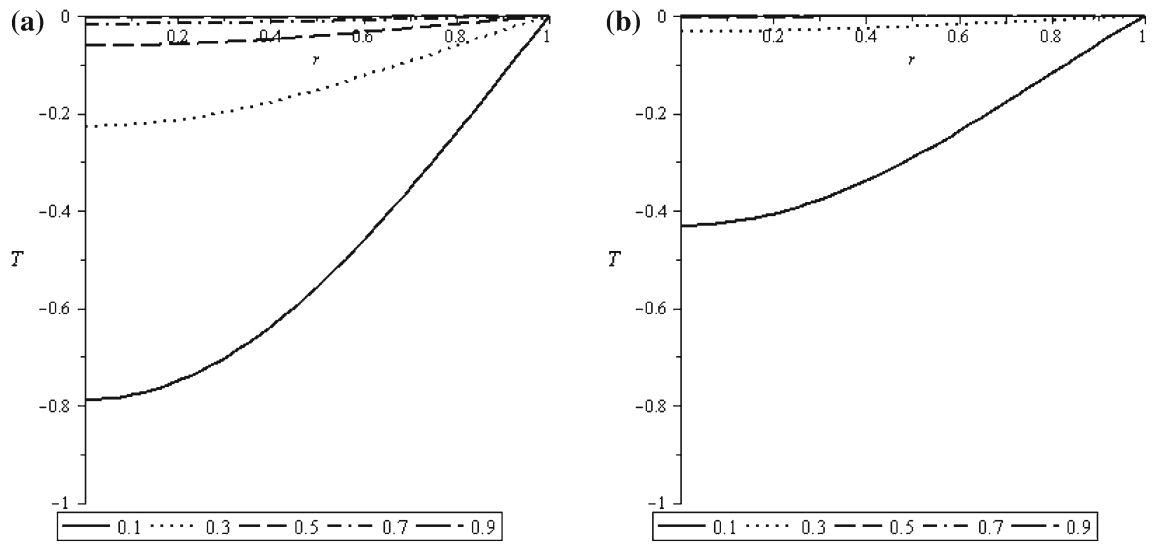

Fig. 2 Dimensionless temperature profiles along the micro-channel for $\kappa R = 79$, $E_z = 5{,}000$, $M = 2.22$, $Re = 0.1$, $Ek = 0$ and $\zeta = 0.5$ at **a** $\Pr = 10$ and **b** $\Pr = 5$

So according to (33), we have the following expression:

$$\theta_n(r,z) = A_n(r)\,B_n(z) = \underbrace{c_{1n}\,c_{2n}}_{c_n}\,f_n(r)\,g_n(z) \tag{41}$$

Constants c_{1n} and c_{2n} can be combined to make a new unknown constant c_n.

Because of linearity of Eq. (28), a linear combination of its solutions is also a solution of (28). Hence, we can write:

$$\theta(r,z) = \sum_{n=1}^{\infty}\theta_n(r,z) = \sum_{n=1}^{\infty} c_n\,f_n(r)\,g_n(z) \tag{42}$$

To determine constant c_n, the third condition of (30) will be applied to the last equation:

$$-1-\phi(r) = \sum_{n=1}^{\infty} c_n\,f_n(r) \tag{43}$$

Then,

$$c_n = \frac{\int_0^1 (-1-\phi(r))w(r)\,f_n(r)}{\int_0^1 w(r)\,(f_n(r))^2} \tag{44}$$

where, $w(r) = r\,V_z$ is the weighing factor, which is found by comparing Eq. (36) with the standard form of Sturm–Liouville equation given below [21]:

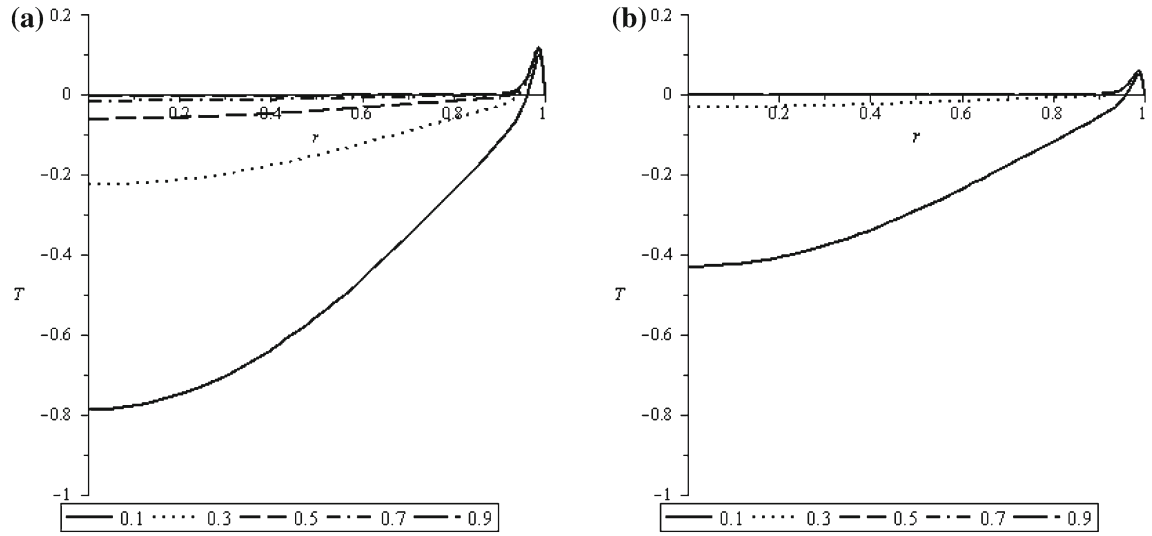

Fig. 3 Dimensionless temperature profiles along the micro-channel for $\kappa R = 79$, $E_z = 5{,}000$, $M = 2.22$, $Re = 0.1$, $Ek = 0.001$ and $\zeta = 0.5$ at **a** Pr = 10 and **b** Pr = 5

$$\frac{\mathrm{d}}{\mathrm{d}r}\left(p(r)\frac{\mathrm{d}u}{\mathrm{d}r}\right) + (q(r) + \lambda\, w(r))u = 0 \tag{45}$$

Therefore, the temperature profile $T(r, z)$ in the thermally developing flow inside a circular micro-channel will be obtained by considering Eqs. (27), (32) and (42). Eigenvalues and some repetitive calculations are made by software Maple.

Once the dimensionless temperature distribution $T(r, z)$ is determined, the local Nusselt number can be obtained as the following dimensionless temperature gradient evaluated at the inner surface of the channel:

$$Nu_z = \left[\frac{\partial T(r, z)}{\partial r}\right]_{r=1} = \frac{T_\mathrm{s} - T_\mathrm{m}(z)}{\Delta T}\left(\frac{h_z R}{k_\mathrm{f}}\right) \tag{46}$$

where, $T_\mathrm{m}(z)$ is the mean fluid temperature.

4 Results

The non-dimensional EDL potential, velocity and temperature profiles, as well as the developing Nusselt number are represented for various conditions. A uniform zeta potential of 12.5 mV is selected for the wall surface (within the bounds imposed by the Debye–Huckel linearization), and a double layer thickness of $4 \times 10^6\,\mathrm{m}^{-1}$ is used in a 40 μ m channel (the channel length is chosen 20 mm). Also, a potential difference of 1 kV/cm is applied along the length of the channel. We consider a $CaCl_2$ aqueous solution at a concentration of 10^{-6} M, $\varepsilon = 80$, $\rho = 1{,}300\,\mathrm{kg/m}^3$, $c_\mathrm{p} = 2{,}500\,\mathrm{J/kg\,K}$, $\alpha = 1.5 \times 10^{-7}\,\mathrm{m}^2/s$ and $\mu = 10^{-3}\,\mathrm{kg/m\,s}$. In the electro-osmotic flow inside the micro-channel, the Reynolds number is usually less than one; so we select two different Reynolds numbers that are much less than unity. To illustrate the essential effects of the viscous dissipation on the temperature profile, a relatively large Eckert number has been used ($Ek = 0.001$).

The dimensionless electrical potential and velocity distributions are shown in Fig. 1 for $\zeta = 0.5$ and two various values of s. The potential field drops off sharply very close to the wall. The region where the net charge density is not zero is limited to a small region close to the channel surface. As illustrated in Fig. 1a, increasing the length scale ratio leads to decreasing the EDL thickness, that is, the EDL potential field falls off to zero more rapidly with distance. As the length scale ratio increases, the velocity field exhibits a profile more similar to plug flow, as shown in Fig. 1b. Generally, in the electro-osmotic flow, the velocity increases rapidly from zero at the wall (shear plane) to a maximum velocity near the wall.

The non-dimensional temperature profiles along the micro-channel are shown in Fig. 2, for $\kappa R = 79$, $E_z = 5{,}000$, $M = 2.22$, $Re = 0.1$, $Ek = 0$ and two various values of Pr. It can be seen that the bulk fluid temperature is gradually increased along the length of the channel. Also, decreasing the Prandtl number results in increasing the dimensionless temperature distribution. This is because diffusion is the prominent mechanism in this type of flow, and therefore the smaller the Prandtl number, the higher the ratio of the thermal diffusion to the thermal advection.

Effect of Eckert number is represented in Fig. 3. Because of the very large velocity and EDL potential gradients close to the channel wall, the contributions of viscous dissipation and electrical field on the temperature distribution near the surface are significant. Hence, the effect of the heat generated by the friction of the fluid shear layers close to the wall is

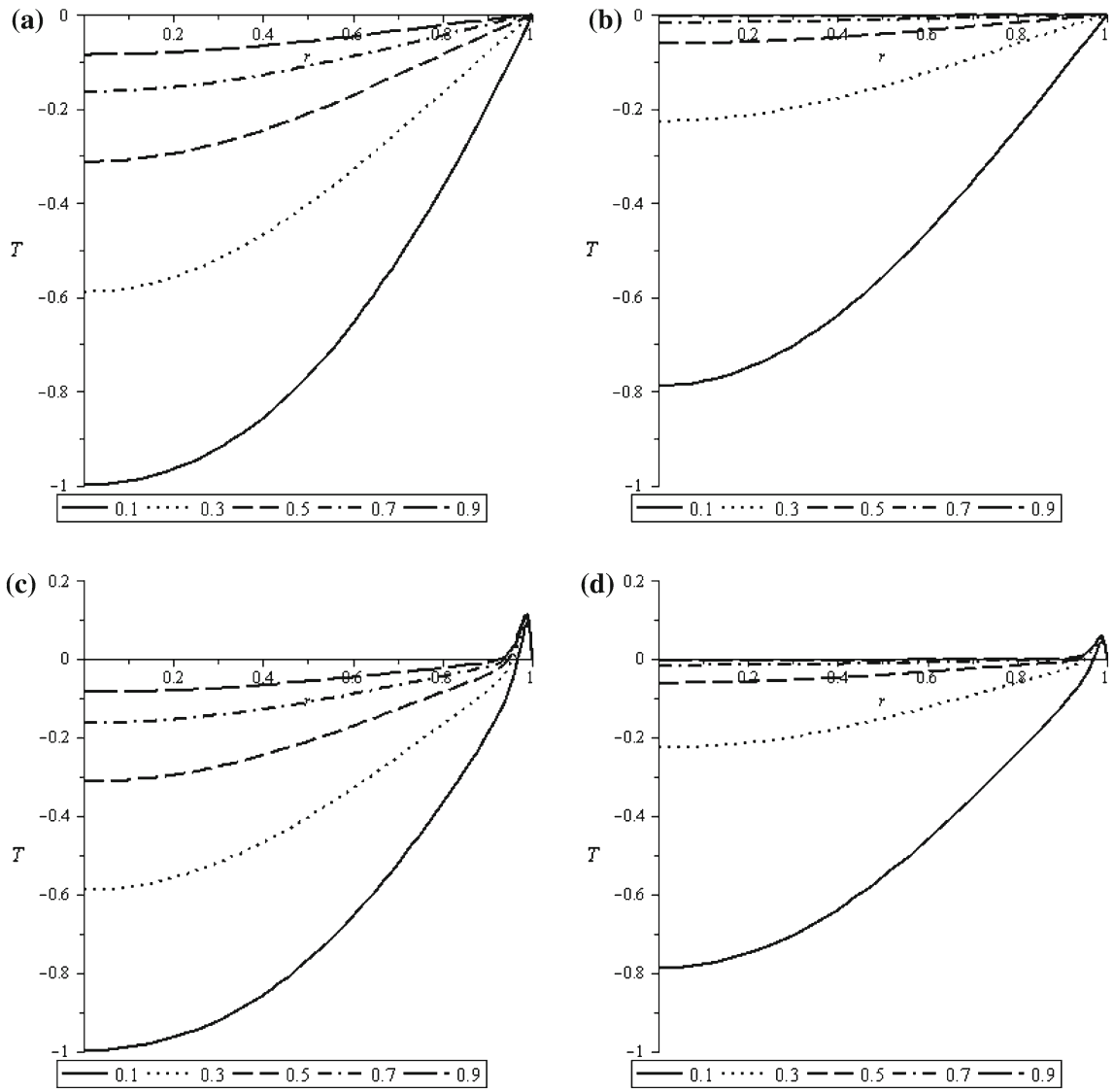

Fig. 4 Dimensionless temperature profiles along the micro-channel for $\kappa R = 79$, $\zeta = 0.5$, $E_z = 5{,}000$, $M = 2.22$ and $Re = 0.2$ at **a** Pr = 10, $Ek = 0$, **b** Pr = 5, $Ek = 0$, **c** Pr = 10, $Ek = 0.001$ and **d** Pr = 5, $Ek = 0.001$

to enhance the near-wall temperature distribution. This heat generation also raises the temperature values of the other portions of the flow field slightly.

The dimensionless temperature profiles for $\kappa R = 79$, $E_z = 5{,}000$, $M = 2.22$, $Re = 0.2$, and two different values of Pr and Ek are shown in Fig. 4, that can be compared with Figs. 2 and 3. The Reynolds number defined in Eq. (23) is proportional to the ratio of the cross-sectional area to length of channel. The increased Reynolds number means the increased ratio of the cross-sectional area to the length of the channel. Compared with Figs. 2, 3, and 4 reveals that the thermal influence of the wall into the flow field will be decreased by increasing the Reynolds number.

Variations of Nusselt number along the micro-channel are represented in Fig. 5, for different values of Prandtl number and Reynolds number. The Nusselt number falls down along the channel in the thermally developing region. This standard trend of Nusselt number also corresponds with the definition presented in Eq. (46).

Figure 6 shows the dimensionless radial heat flux near the wall for $\kappa R = 79$, $\zeta = 0.5$, $E_z = 5{,}000$, $M = 2.22$, $Re = 0.1$, Pr = 5 and two different values of z. The dimensionless radial heat flux is calculated by $-\partial T(r, z)/\partial r$. The absolute value of radial heat flux decreases along the micro-channel, since the bulk temperature gradually approaches the constant surface temperature. As defined here, the constant surface temperature is higher than the bulk fluid temperature, hence, without considering the viscous heating, the radial heat flux vector is toward the channel centerline (i.e., its sign is negative). But the enhanced temperature near the wall due

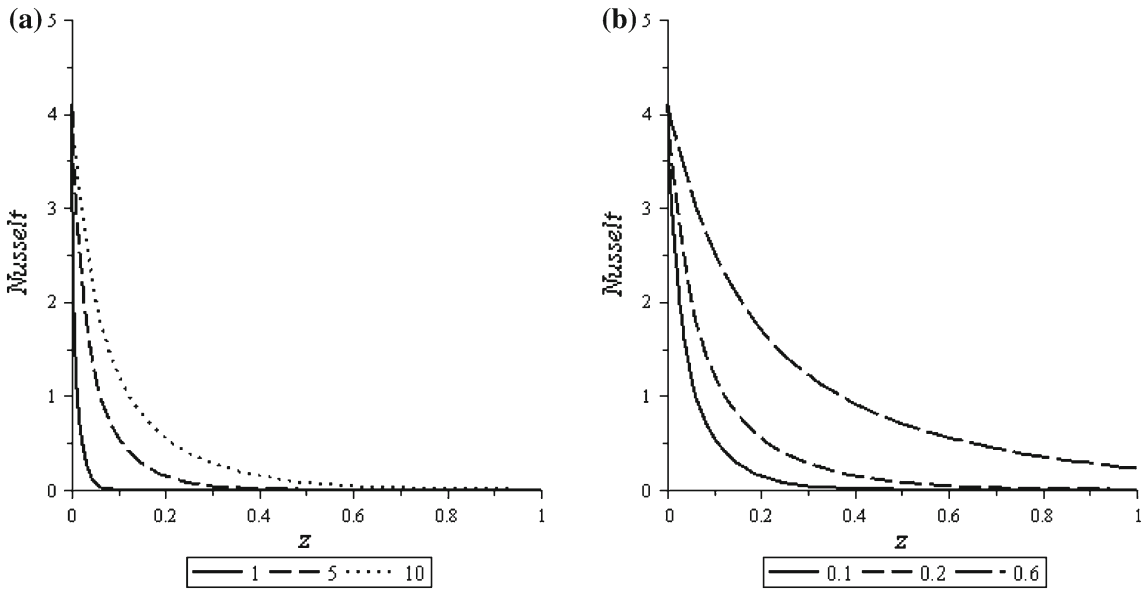

Fig. 5 Variations of Nusselt number along the micro-channel for $\kappa R = 79$, $\zeta = 0.5$, $E_z = 5{,}000$, $M = 2.22$, and $Ek = 0$ at **a** $Re = 0.1$ and different values of Pr, and **b** $\mathrm{Pr} = 5$ and different values of Re

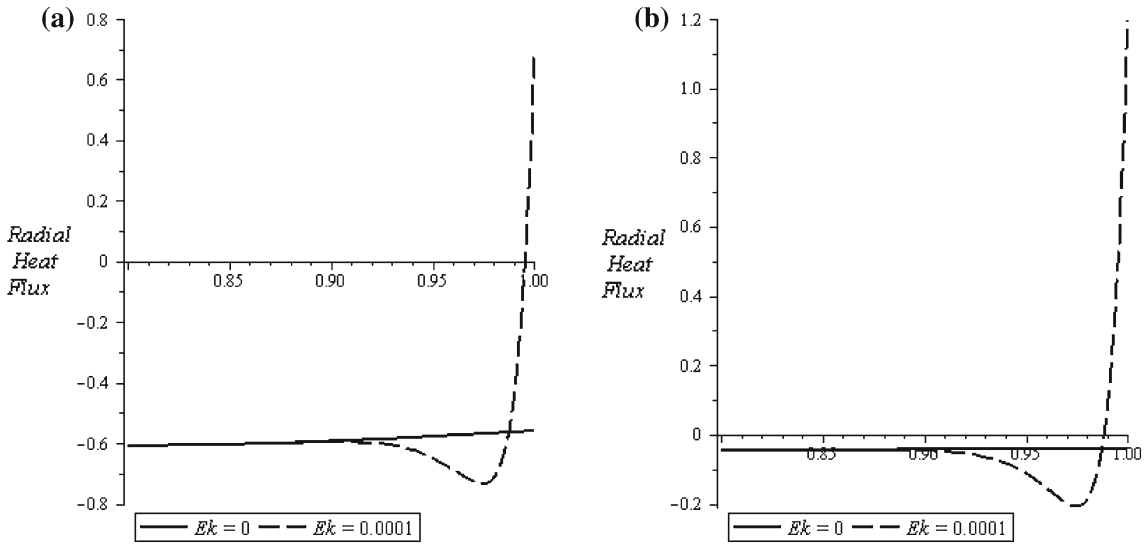

Fig. 6 Dimensionless radial heat flux near the wall for $\kappa R = 79$, $\zeta = 0.5$, $E_z = 5{,}000$, $M = 2.22$, $Re = 0.1$, and $\mathrm{Pr} = 5$ at **a** $z = 0.1$ and **b** $z = 0.3$

to the viscous dissipation leads to a radial heat flux with a positive sign near the wall.

5 Conclusion

In the present study, an analytical analysis based on the linearized Poisson–Boltzmann equation has been developed for liquid flow and associated heat transfer in a circular microchannel at symmetric electrostatic, kinematic, and thermal boundary conditions.

The unique plug-like velocity profile can be attributed to the fact that the externally imposed electrical field is driving the flow. This situation may be seldom seen in the pressure-driven flows. In the mobile part of the EDL region very close to the wall, the larger electrical field force exerts a greater driving force on the fluid because of presence of the net charge in the EDL region. The surface electric condition of zeta potential influences the electric potential distribution directly and alters flowing potential as well as the liquid hydrodynamic and thermal characteristics. Effects of Reynolds and Prandtl numbers, as well as the viscous dissipation, on the flow field thermal characteristics are represented and discussed. An interesting phenomenon that can be seen clearly near the channel wall is the increased temperature due to the very large velocity gradient close to the wall

surface, which acts like a heat generation source. Decreasing the Nusselt number in the thermally developing region is also represented. The positive radial heat flux near the channel wall may be observed due to the relatively large viscous heating.

Acknowledgments This work was supported by Shahrood University of Technology through a research grant.

References

1. Kandlikar, S.; Garimella, S.; Li, D.; Colin, S.; King, M.R.: Heat Transfer and Fluid Flow in Minichannels and Microchannels. Elsevier, Oxford (2006)
2. Anderson, J.L.: Effect of nonuniform zeta potential on particle movement in electric fields. J. Colloid Interface Sci. **105**, 45–54 (1985)
3. Arulanandam, S.; Li, D.: Liquid transport in rectangular microchannels by electroosmotic pumping. Colloid Surface A **161**, 89–102 (2000)
4. Erickson, D.; Li, D.: Analysis of AC electroosmotic flows in a rectangular microchannel. Langmuir **19**, 5421–5430 (2003)
5. Wang, M.; Chen, S.: Electroosmosis in homogeneously charged micro- and nanoscale random porous media. J. Colloid Interface Sci. **314**, 264–273 (2007)
6. Dutta, P.; Beskok, A.: Analytical solution of combined electroosmotic/pressure driven flows in two-dimensional straight channels: finite Debye layer effects. Anal. Chem. **73**, 1979–1986 (2001)
7. Dutta, P.; Beskok, A.: Analytical solution of time periodic electroosmotic flows: analogies to stokes second problem. Anal. Chem. **73**, 5097–5102 (2001)
8. Soderman, O.; Jonsson, B.: Electro-osmosis: velocity profiles in different geometries with both temporal and spatial resolution. J. Chem. Phys. **105**, 10300–10311 (1996)
9. Moghadam, A.J.: An exact solution of AC electro-kinetic-driven flow in a circular micro-channel. Eur. J. Mech. B/Fluids **34**, 91–96 (2012)
10. Soong, C.Y.; Wang, S.H.: Theoretical analysis of electrokinetic flow and heat transfer in a microchannel under asymmetric boundary conditions. J. Colloid Interface Sci. **265**(1), 202–213 (2003)
11. Xuan, X.; Li, D.: Thermodynamic analysis of electrokinetic energy conversion. J. Power Sour. **156**, 677–684 (2006)
12. Wang, M.; Kang, Q.: Modeling elctrokinetic flows in microchannels using coupled lattice Boltzmann methods. J. Comput. Phys. **229**, 728–744 (2010)
13. Tang, G.H.; Li, X.F.; Tao, W.Q.: Microannular electro-osmotic flow with the axisymmetric lattice Boltzmann method. J. Appl. Phys. **108**(11), 114903 (2010)
14. Xuan, X.C.; Li, D.: Electroosmotic flow in microchannels with arbitrary geometry and arbitrary distribution of wall charge. J. Colloid Interface Sci. **289**, 291–303 (2005)
15. Sadeghi, A.; Saidi, M.H.: Viscous dissipation effects on thermal transport characteristics of combined pressure and electroosmotically driven flow in microchannels. Int. J. Heat Mass Transf. **53**, 3782–3791 (2010)
16. Maynes, D.; Webb, B.W.: Fully developed electro-osmotic heat transfer in microchannels. Int. J. Heat Mass Transf. **46**, 1359–1369 (2003)
17. Yang, C.; Li, D.; Masliah, J.H.: Modeling forced liquid convection in rectangular microchannels with electrokinetic effects. Int. J. Heat Mass Transf. **41**, 4229–4249 (1998)
18. Nguyen, N.Y.; Wereley, S.T.: Fundamentals and Applications of Microfluidics. ARTECH HOUSE, Boston (2006)
19. Hardt, S.; Schonfeld, F.: Microfluidic Technologies for Miniaturized Analysis Systems. Springer, New York (2007)
20. Spiegel, M.R.; Lipschutz, S.; Liu, J.: Mathematical Handbook of Formulas and Tables. McGraw-Hill, NY (2009)
21. Arfken, G.: Mathematical Methods for Physicists. ACADEMIC PRESS, Orlando (1985)